Research Square

Preprints are preliminary reports that have not undergone peer review.
They should not be considered conclusive, used to inform clinical practice,
or referenced by the media as validated information.

Thermal stratification characterisation of large tunnel fires under forced ventilation

Nigel Charles Dhlamini

dhlnig001@myuct.ac.za

University of the Witwatersrand

Reshendren Naidoo

University of the Witwatersrand

Wei Hua Ho

University of Cape Town

Research Article

Keywords: stratification stability, thermal buoyancy, Froude number, tunnel fire, smoke behaviour, large fires

Posted Date: March 23rd, 2026

DOI: https://doi.org/10.21203/rs.3.rs-9048432/v1

License: This work is licensed under a Creative Commons Attribution 4.0 International License.
Read Full License

Additional Declarations: No competing interests reported.

Thermal stratification characterisation of large tunnel fires under forced ventilation

Abstract

Large tunnel fires exhibit thermal stratification dynamics that are distinct from small fires, yet most existing correlations for smoke stratification are derived from small-scale or reduced-scale experiments. This computational study investigates thermal stratification in tunnels using two high-intensity fires (30 MW and 80 MW) under varying ventilation velocities. Unlike previous research that assumes ambient floor temperatures, the results show that large fires generate floor temperatures significantly above ambient due to radiative heat transfer from the extended ceiling flame. The critical temperature ratio for stable stratification was found to be $\Delta T_{cf}/\Delta T_{avg} = 1.9$, compared to the traditional value of 1.7, with a corresponding critical Froude number of 0.858. A new empirical correlation relating the temperature ratio to the Froude number is proposed and compared against existing correlations from the literature. The discrepancy in critical Froude numbers reported across previous studies is discussed, and the limitations of the Froude number as a sole descriptor of stratification stability in large fires are highlighted.

Keywords: stratification stability, thermal buoyancy, Froude number, tunnel fire, smoke behaviour, large fires

1 Introduction

Fire in a mine or transportation tunnels is a serious hazard that could result in a significant loss of lives. Mines contain significant amounts of flammable materials such as fuel (inside and outside mine vehicles), hydraulic oil, lubricants, timber, rubber, plastics, paints and packaging materials. There also exist numerous potential ignition sources such as flame from cutting and welding equipment, sparks, electrical short circuits, and hot surfaces on machinery.

The global mining industry has experienced several underground fire incidents such as the Benxihu (Honkeiko) coal mine incident in China which claimed over 1,500 lives in 1942 [1]. South Africa also has had its share of unfortunate underground fire incidents such as the Kinross gold mine disaster in 1986 which killed 177 people [2].

Smoke from a fire contains combustion products such as carbon monoxide and other asphyxiant and irritant gases which, when inhaled, are hazardous. Thermal buoyancy is the tendency of warm air or smoke to rise in cooler surrounding air. When this

happens, there is clear and stable stratification which creates a tenable region where evacuation can take place near to the floor of the tunnel. However, this stratification can sometimes be destroyed when there is high ventilation velocities and this makes evacuation very difficult and puts tunnel occupants in grave danger.

Thermal buoyancy and inertia force are the two main factors that affect the stability of fire-induced thermal stratification [3]. Forced ventilation-induced inertia force tends to mix the flow, while buoyancy maintains the stability of the stratification. Newman [4] was the first to investigate the phenomenon of fire-induced thermal stratification in tunnel fires in 1984 and conducted experiments to simulate conditions in an underground mine passage in the presence of fire and ventilation flow. He used vertical temperature variation as a proxy for smoke stratification and used three different temperature differences to characterise his findings.

- ΔT_{cf} - the local vertical temperature difference between the ceiling and the floor.
- ΔT_{avg} - the local temperature difference between the vertical average temperature and the ambient temperature. The vertical average temperature is calculated from temperature measurements taken between the ceiling and the floor at a longitudinal location of interest, downstream of the fire.
- ΔT_h - the local temperature difference between the ceiling and the ambient temperature.

Ambient temperature refers to the temperature in the tunnel before a fire occurs and can be assumed to be the same as the temperature far upstream of the fire.

Newman [4] found that there exists two distinct regions of stratification which he characterised using two ratios, $(\Delta T_{cf}/\Delta T_{avg})$ and $(\Delta T_{cf}/\Delta T_h)$. At Region 1, the temperature at the floor is close to ambient and the smoke is fully stratified and $(\Delta T_{cf}/\Delta T_h) = 1$. Stratification gradually weakens as the floor temperature rises in Region 2 and $(\Delta T_{cf}/\Delta T_h) < 1$.

Froude Number is the ratio of the inertia force to the buoyancy force and is often used to characterise fire-induced thermal stratification [5, 6]. Generally, the weakly stratified regime will have a high Froude number, and the strongly stratified regime will have a low Froude number. Fr-based parameterisation implicitly suggests that the background influences of the inertia force and thermal buoyancy determine stratification stability. Based on the Froude number, Newman [4] refined the two regions described above and proposed three smoke stratification regions (see Fig. 1). For ease of reference, they will be renamed Regions A, B and C. Region A ($Fr \leq 0.9$) is approximately the same as Region 1 and Regions B and C with Region 2. The difference between Regions B and C lies in the level of stratification (or mixing), where although the floor temperature no longer ambient, some evidence of stratification still exists in Region B ($0.9 < Fr < 10$) but is completely absent in Region C ($Fr \geq 10$) as the flow becomes fully mixed. Newman [4] proposed an empirical correlation between $(\Delta T_{cf}/\Delta T_{avg})$ and Froude Number (Fr), shown in Eq. (1):

$$\Delta T_{cf}/\Delta T_{avg} = 1.5 Fr^{-1} \tag{1}$$

Where Fr was defined as follows:

$$Fr = \frac{u_{avg}}{\sqrt{gh\Delta T_{cf}/T_{avg}}}, \qquad u_{avg} = \frac{u_0 T_{avg}}{T_0}$$

h is the height of the channel, u_0 is the longitudinal ventilation velocity, and T_0 is the ambient temperature.

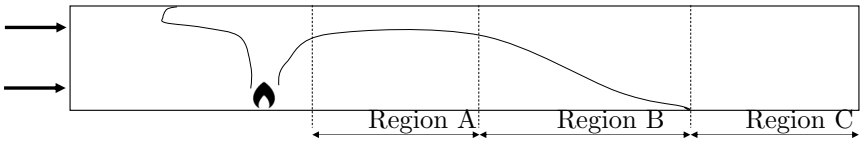


Fig. 1: Newman [4]'s Smoke Stratification Regions.

The critical Froude number (Fr_c) delineates between stratification regimes, i.e. between Region 1 and Region 2, and therefore can be understood to describe stratification stability. Given that Froude number defines a balance between inertia force and buoyancy force it should follow that at the transition between regimes the Froude number should be near unity, when the background influence of buoyancy force would then be taken over by shear force. However, most studies reported here found a critical Froude number that is different from the expected $Fr \approx 1$.

Following Newman [4]'s work, Nyman and Ingason [7] analysed full-scale and model-scale fire tests to validate this theory and criteria for smoke stratification. In their analysis the relationship between temperature ratio and Froude number was different from that in Eq. (1). They instead proposed the correlation in Eq. (2). Newman [4]'s experiment was performed in a duct, whereas Nyman and Ingason [7] analysed data from large-scale tunnel fire tests, as well as model-scale tests that made use of Froude number scaling.

$$\frac{\Delta T_{cf}}{\Delta T_{avg}} = 0.62 Fr^{-1.58} \tag{2}$$

A number of further studies were conducted to characterise $\Delta T_{cf}/\Delta T_{avg}$ and Fr but on slightly different scenarios and they came up with different correlations. For instance, Li et al. [8] performed reduced-scale experiments to explore the smoke thermal stratification with ceiling extraction in a longitudinal ventilation tunnel, and proposed Eq. (3) by fitting experimental data. Huang and Li [9] investigated the smoke stratification characteristics of corridor fires under the action of outdoor natural wind flowing into the corridor, and found that Fr and $\Delta T_{cf}/\Delta T_{avg}$ have the relationship shown in Eq. (4). The study revealed that external wind diminishes smoke stratification within the corridor, and the stability of smoke stratification heightens with rising heat release rate (HRR) and thermal buoyancy but diminishes with larger window sizes. Guo et al. [10] derived Eq. (5) through fitting simulation data, aiding in discerning smoke stratification downstream of tunnel fires under longitudinal ventilation.

Yang et al. [11] employed Eq. (6) to fit data from fire tests conducted on a 1:20 scale tunnel platform. The critical criterion for determining whether the smoke stratification is in Region 1 (highly stratified, no interfacial mixing) is $\Delta T_{cf}/\Delta T_{avg} = 1.8$ in the study by Huang and Li [9], however, in most other studies it is $\Delta T_{cf}/\Delta T_{avg} = 1.7$ [4, 7, 8, 10].

$$\frac{\Delta T_{cf}}{\Delta T_{avg}} = 0.67 Fr'^{-1.54} \tag{3}$$

$$\frac{\Delta T_{cf}}{\Delta T_{avg}} = 70.43 \exp\left[-\left(\frac{Fr + 4.357}{2.427}\right)^2\right] \tag{4}$$

$$\frac{\Delta T_{cf}}{\Delta T_{avg}} = 0.84 Fr^{-1} \tag{5}$$

$$\frac{\Delta T_{cf}}{\Delta T_{avg}} = a b^{Fr} \tag{6}$$

where a was found to have an average value of 3.26 an b and average value of 0.68 [11].

Key findings for these studies including the seminal work of Newman [4] are summarised and presented in Table 1 with their different critical Froude numbers.

Table 1: Critical Froude Number

Critical Froude Number	Reference
0.29	Huang and Li [9]
0.49	Guo et al. [10]
0.55	Nyman and Ingason [7], and Li et al. [8]
0.90	Newman [4]
1.63	Yang et al. [11]

It is evident that there exists a discrepancy in several past work on how to describe the thermal stratification status of smoke in tunnel fires, shown by the disagreement between critical Froude numbers. This could partly be explained by the different experiment conditions in different studies. In some tests the fire development was transient and in others steady state. This has a direct effect on the temperature and velocity profiles, which would directly affect Froude number. Additionally, most of these studies operate in the small fire range, particularly evidenced by the assumption that floor temperature is the same as ambient temperature, and extrapolating these results to large fires is non-trivial which is what this current study seeks to address. In this study we use numerical simulations and pay particular attention to large tunnel fires, whose physical mechanism for smoke movement and stratification is different from that of small fires. When the fire is large the flame tip impacts the ceiling and the combustion zone spreads along the tunnel ceiling. A large tunnel fire is defined as having a dimensionless heat release rate (Q^*) of over 0.15, where the dimensionless heat release

rate $Q^* = \dot{Q}/(\rho_a c_p T_a g^{1/2} h^{5/2})$, and the other terms have their usual meaning. In an open fire, the flame and hot gases radiate heat to the surroundings with minimal heat feedback. Conversely, in a large tunnel fire, heat feedback significantly influences the heat balance between flames and hot gases, while forced ventilation enhances combustion. This dynamic typically results in a fuel-controlled fire within a well-ventilated tunnel, leading to higher temperatures of flames and hot gases compared to those in open fires or building enclosures [12]. It is therefore important to explore large tunnel fires as they would be driven by different physical mechanisms to small tunnel fires.

2 Numerical Method

The simulated tunnel was 150m long, 10m wide, and had a height of 5m and is shown in Fig. 2. The heat release rates that were simulated were 30 MW and 80 MW, which can be categorised as large fires ($Q^* = 49.5$ for the 30MW fire, and $Q^* = 132$ for the 80MW fire).

The inlet and outlet ends of the tunnel were velocity inlet and pressure outlet boundaries, respectively. The fire source was located 20m from the tunnel inlet, to allow for some smoke flow upstream and also for the flow to be fully developed downstream.

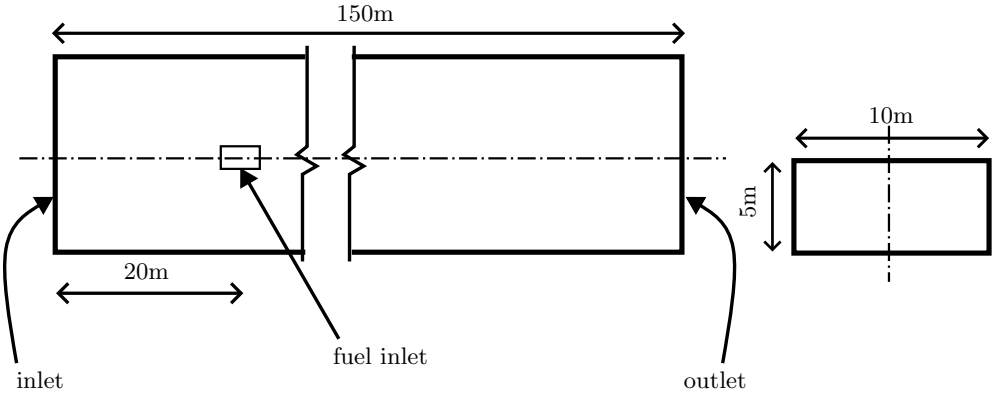


Fig. 2: Computational Domain. (a) Tunnel longitudinal section (top). (b) Tunnel cross-section.

Li et al. [13] and Ingason et al. [14] have found that selecting a grid size of $0.075D^*$, where D^*, the characteristic fire diameter, calculated as shown in Eq. (7), is reasonable for a tunnel fire simulation. The ratio of the characteristic fire diameter to the nominal mesh size, $D^*/\Delta x$, should be between 4 and 16 to fully resolve plume dynamics, where a low number represents a coarse grid and a high number a fine grid size [15].

$$D^* = \left(\frac{\dot{Q}}{\rho_a c_p T_a \sqrt{g}} \right)^{2/5} \tag{7}$$

A structured mesh approach was used because of the simplicity of the geometry and the quasi-steady nature of the flow, with a little over 3,500,000 cells. The grid had a $D^*/\Delta x$ of 6, calculated according to Eq. (7), and a finer grid resolution ($D^*/\Delta x = 12$) was used where strong local gradients of properties were expected. A final time-step size of 0.05s and courant number of 1 were used.

The turbulence model used is based on the conceptual framework provided by the Reynolds-averaged form of the Navier–Stokes equations (RANS), in particular the realizable $k - \epsilon$ turbulence model proposed by Shih et al. [16]. The uncoupled implementation of the Discrete Ordinates (DO) radiation model was used and it is sequential in nature and uses a conservative variant of the DO model called the finite-volume scheme [17].

2.1 Boundary Conditions and Initial Conditions

The initial conditions assumed a temperature of $300K$ and a pressure of $101.325kPa$ in the tunnel as the ambient conditions. Tiny amounts of the combustion products were also initiated into the domain to trigger combustion (see Eq. (11)), with mass fractions of both the carbon dioxide and the water vapour being 1×10^{-10}.

The boundary conditions are shown in Fig. 2. An assumption was made that the materials of the tunnel surface including walls, ceilings and floors were concrete. These were set in ANSYS Fluent as WALL boundaries. Tunnel walls were modelled as hydraulically smooth. A two-layer model and enhanced wall functions were combined to account for the effect of wall roughness on momentum and heat transfer. The inlet was set a VELOCITY INLET and the outlet as a PRESSURE OUTLET at ambient pressure. The location of the fire source was at [20, 0, 0]m. The centre of the fire is taken as the origin, the $x - axis$ defines the longitudinal direction of the tunnel: x is negative upstream of the fire source and positive downstream. The fire source was set to a steady-state fire.

The tunnel was divided through its length-wise central axis to reduce computational expense and a SYMMETRY boundary condition was imposed in the mid-plane. The assumption of a symmetry boundary was made based on previous work [18] which showed that smoke flow develops in a fairly symmetrical manner, so the boundary condition would not interfere with the development of physical mechanisms in smoke propagation.

2.2 Combustion Model

The reacting flow methodology presented here does not attempt to directly model the actual, complicated combustion scenario, which, if modelled, would result in high computational expense and runtime. Instead there is a continuous addition of fuel at the fire location, akin to gradual release of vapour. The heat release rate of the fire is fairly constant over the lifetime of the simulation and the velocity and temperature of the flow are quasi-steady, which results in well-ordered flow. The combustion process can generally be divided into four stages: initial stage, growth stage, steady profile or developed phase, and decay stage. The stage simulated in this present study is the

steady profile or developed phase, corresponding to the fully developed fire after flash-over. In this phase, the heat release rate is at its peak value, representing the worst case scenario.

The most basic description of the chemistry of fire is a reaction of a hydrocarbon fuel with oxygen that produces carbon dioxide and water vapour. Propane was used as the fuel, chosen for its nature as a hydrocarbon that could be used for gaseous combustion. Propane was assigned different mass loss rates ($\dot{m}_f$) at the fuel inlet (calculated as shown in Eq. (8)), prescribed according to the desired fire size.

$$\dot{m}_f = \frac{\dot{Q}}{\mathcal{X} \cdot \Delta H_c} \tag{8}$$

Where $\mathcal{X}$ is the combustion efficiency, ΔH_c is the heat of combustion, and $\dot{Q}$ is the desired heat release rate.

In the present study the combustion process was simplified, the chemistry was treated by the irreversible single step mechanism given in Eq. (9):

$$C_3H_8 + 5(O_2 + 3.76N_2) \rightarrow 3CO_2 + 4H_2O + 18.8N_2 \tag{9}$$

The Species Transport Equations and Eddy Dissipation Model (EDM) were used to model the turbulence/chemistry interaction. The EDM was developed by Magnussen and Hjertager [19] and it computes the reaction rates based on turbulent mixing. The assumption is that the chemical kinetic rates are a lot faster than rates of turbulent mixing, so the rate-limiting process is turbulent mixing. The net rate of production of species, i, due to reaction, r, $R_{i,r}$ is given by the limiting value of the two expressions shown in Eq. (10) and Eq. (11). The chemical reaction rate is governed by the large eddy mixing time scale, $\frac{\epsilon}{k}$, whenever turbulence is present ($\frac{\epsilon}{k} > 0$).

A source of ignition was not a requirement for combustion to occur, instead a small amount of the products were patched into the flow field to initiate the reaction as shown in Eq. (11) [19], with mole fractions of 1×10^{-10} for both H_2O and CO_2.

$$R_{i,r} = \nu_{i,r}^{'} M_{w,i} A \rho \frac{\epsilon}{k} min_{\mathcal{R}} \left(\frac{Y_{\mathcal{R}}}{\nu_{\mathcal{R},r}^{'} M_{w,\mathcal{R}}} \right) \tag{10}$$

$$R_{i,r} = \nu_{i,r}^{'} M_{w,i} A B \rho \frac{\epsilon}{k} \frac{\sum_P Y_P}{\sum_j^N \nu_{j,r}^{''} M_{w,j}} \tag{11}$$

Where Y_P is the mass fraction of any product species, P. $Y_{\mathcal{R}}$ is the mass fraction of a particular reactant, $\mathcal{R}$. A is an empirical constant equal to 4. B is an empirical constant equal to 0.5.

The time scale of the reaction is much shorter than the flow time, therefore it can generally be acceptable to approximate the chemical reaction as infinitely fast, and so combustion is mixing-limited.

A number of simulations were undertaken and are shown in Table 2. The choice of the ventilation velocities is based on normal airflow requirements in a mine which are

between 0.5 m/s and 1.5 m/s [20], and smoke stratification requirements for airflow which are up to 3 m/s [21]. The fire sizes chosen are based on vehicle fires (≈30MW) and diesel tank fires (≈80MW), which are design fires for hard-rock mines as discussed in Hansen [22].

Table 2: Simulation Scenarios Undertaken

Fire Size (HRR) [MW]	Ventilation Velocity [m/s]
30	1, 2, 3, 4
80	1, 2, 3, 4

2.3 Verification and Validation

The grid size was initially found using the empirical model in Eq. (7) as 0.1 m but a grid independence study was undertaken to confirm mesh insensitivity and the results are shown in Table 3. The solution on the finest grid had a quantity of interest of 327K, and the extrapolated value is 316.7K, that is not too far off, which is also supported by a low GCI value of 3.93% going from Grid 2 to Grid 1. Grid 2, with a cell size of 0.1 m, was then confirmed and used in this study.

Table 3: Grid convergence study over 4 grids. ϕ represents the quantity of interest ΔT_{avg} and $\phi_{extrapolated}$ its Richardson extrapolated value. h is the representative grid spacing, r the refinement ratio between two successive grids. GCI is the grid convergence index in percent and its asymptotic value is provided by $GCI_{asymptotic}$, where a value close to unity indicates a grid independent solution. The order achieved in the simulation is given by p.

Grid	h [m]	r	ϕ	GCI [%]	$GCI_{asymptotic}$	p	$\phi_{extrapolated}$
Grid 1	0.05	–	327	3.93%	0.849	1.074	316.7
Grid 2	0.10	2.0	340	7.56%	–	1.284	319.4
Grid 3	0.25	2.5	380	21.6%	–	–	–
Grid 4	0.50	2.0	463	–	–	–	–

Some performance parameters were tracked for verification of the model according to the physics of the scenario, including the courant number, the radiative heat transfer at the walls, the total heat flux in the domain, the carbon dioxide concentration at the domain outlet and the temperature at the tunnel outlet. These all indicated that the flow reached sufficient pseudo-steady conditions in the simulated 120s.

The predictive capabilities of RANS simulations are subject to structural uncertainties inherent in the turbulence model [23]. Confined buoyancy-induced turbulent flows emanating from a heat source or a fire have been studied using various adjusted

forms of the $k-\epsilon$ turbulence model [24–27], with reasonable predictions of turbulence quantities near and far from the wall [28, 29]. While scale-resolving approaches such as DNS or LES would ideally avoid these limitations, they remain prohibitively expensive for high Reynolds number wall-bounded flows such as those in tunnels. Consequently, the realizable $k-\epsilon$ turbulence model with enhanced wall treatment (including pressure gradient and thermal effects) was adopted here, with the model constants kept at their standard values ($C_{2\epsilon} = 1.9$, turbulent Prandtl numbers $\sigma_k = 1$ and $\sigma_\epsilon = 1.2$, energy and wall Prandtl numbers = 0.85, and turbulent Schmidt number = 0.7), as these are well-established in this context.

Wall functions were applied consistently with the near-wall mesh design ($y^+ \approx 30 - –300$) to ensure compatibility with the logarithmic boundary layer region where heat transfer is dominant. Representative ceiling and floor temperatures were taken at $y_c = 0.88H$ and $y_f = 0.12H$, following established practice in enclosed fire studies [4], ensuring that wall heat transfer was not arbitrarily imposed but grounded in empirical conventions.

To provide confidence in these modelling choices, a validation exercise was carried out by simulating a 60 kW tunnel fire based on Li et al. [8] and comparing against experimental temperature stratification and ceiling jet data from Nyman and Ingason [7] and Li et al. [8]. The comparison, shown in Fig. 3, demonstrates good agreement in the slope of $\Delta T_{cf}/\Delta T_{avg}$ versus Froude number generally agreeing with that of Eq. 2, indicating that the chosen turbulence model and wall function treatment capture the dominant heat transfer mechanisms relevant to the present study.

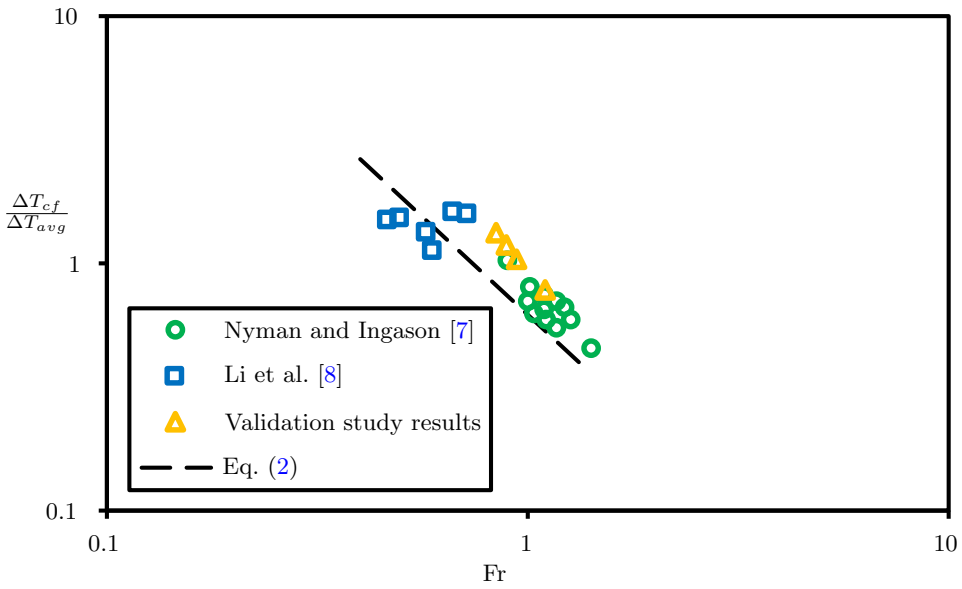


Fig. 3: The temperature ratio $\Delta T_{cf}/\Delta T_{avg}$ versus Froude number, showing the validation set from this study with previous experimental data.

3 Results and Discussion

3.1 Thermal Stratification Status

Newman [4] found that the vertical temperature distribution can reflect the smoke stratification state. The data revealed two regions: Region 1 characterised by $(\Delta T_{cf}/\Delta T_{avg}) > 1.7$, and Region 2 given by $(\Delta T_{cf}/\Delta T_{avg}) \leq 1.7$. For Region 1, $(\Delta T_{cf}/\Delta T_h) \approx 1$, which implies that the flow near the floor is at ambient temperature.

Data from this study were plotted to find the relationship between $\Delta T_{cf}/\Delta T_{avg}$ and $\Delta T_{cf}/\Delta T_h$, and those results are shown in Fig. 4 and Fig. 5. The results in Fig. 4 generally deviate from Newman's work. A new correlation was then fitted to more accurately represent these results and it is stated in Eq. (12). The disagreement between the current study and Newman [4]'s work can be explained by the fire sizes simulated here. When a high intensity fire or a large fire occurs, the flow near the floor in the near-field region of the fire location will not be at ambient temperature, even if the smoke is stably stratified.

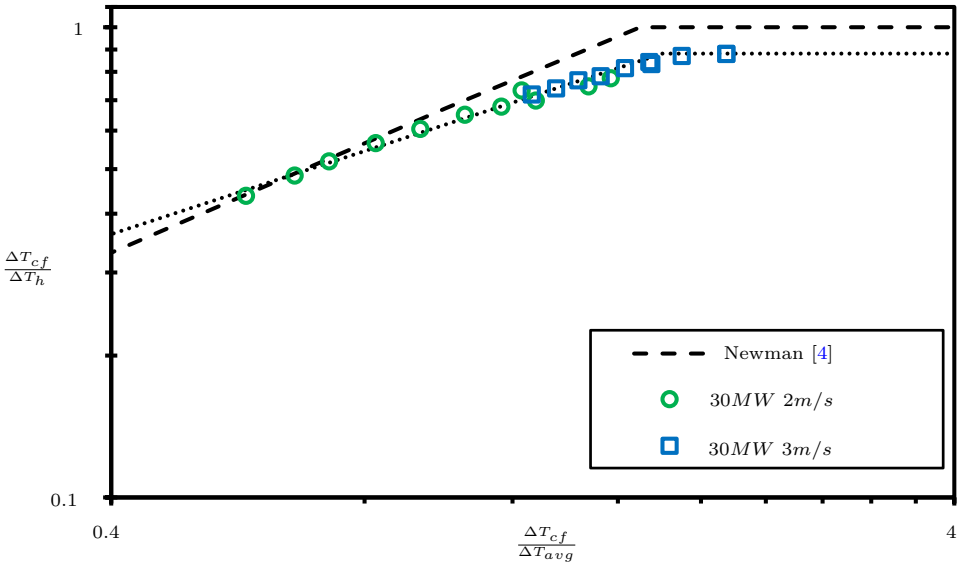


Fig. 4: Gas Temperature Stratification, 30MW Fire.

However, in Fig. 5 data from the 80MW fire follow the new correlation in Eq. (12) while in Region 1, but then are represented more accurately by Newman [4]'s correlation in Region 2.

$$\frac{\Delta T_{cf}}{\Delta T_h} = 0.62 \left(\frac{\Delta T_{cf}}{\Delta T_{avg}} \right)^{0.59}, \qquad \frac{\Delta T_{cf}}{\Delta T_{avg}} < 1.9$$

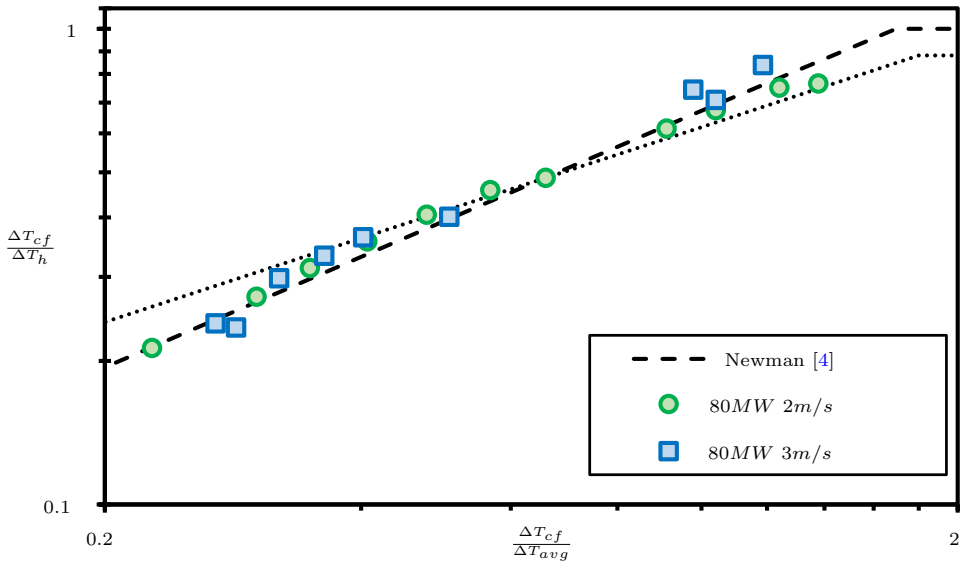


Fig. 5: Gas Temperature Stratification, 80MW Fire.

$$\frac{\Delta T_{cf}}{\Delta T_h} = 0.875, \qquad \frac{\Delta T_{cf}}{\Delta T_{avg}} \geq 1.9 \tag{12}$$

Region 1 in the current study is characterised by $\Delta T_{cf}/\Delta T_h \approx 0.875$. What is of importance is that the temperature ratio is less than 1 because the temperature at the floor is higher than ambient for large fires, which means $\Delta T_{cf} < \Delta T_h$. The critical value of $\Delta T_{cf}/\Delta T_{avg}$ for describing stratification is therefore 1.9, as opposed to 1.7 [4, 7, 8, 10] or 1.8 [9]. Radiative transport is an important mechanism for heat transfer in a convective-diffusive-reactive environment, especially one created by a large fire, such that the space heating of quiescent air as the fire plume rises will raise its temperature above ambient conditions. As the resident air temperature increases, the difference between ceiling and floor temperatures, which gives plume buoyancy, decreases and this can lead to limited plume rise. The physical mechanism of heat and smoke flow in the near-field of the fire location for a large fire must therefore scale up spatially and temporally from that for a small fire.

It is important to note that the critical criterion for stable stratification $\Delta T_{cf}/\Delta T_{avg} = 1.7$ in previous work [4, 7, 8, 10] was obtained empirically and has no physical reference. If it were to be calculated analytically, assuming the temperature at the floor is ambient temperature (for clear stratification) and the average temperature $T_{avg} \approx (T_c + T_f)/2$:

$$\frac{\Delta T_{cf}}{\Delta T_{avg}} = \frac{T_c - T_f}{T_{avg} - T_a} \approx \frac{T_c - T_a}{\frac{T_c + T_a}{2} - T_a} = \frac{2(T_c - T_a)}{T_c - T_a} = 2$$

This analytical value is closer to the 1.9 found in this study. Where T_a is the ambient temperature, T_c is the temperature at the ceiling, and T_f is the temperature at the floor.

3.2 Stratification Status using Froude Number

The Froude number distribution along the length of the tunnel, downstream of the fire location is shown in Fig. (6) for different ventilation velocities for a 30MW fire. Overall, the Froude number increased with the increase in longitudinal velocity. The Froude number downstream of the fire gradually increased in the longitudinal direction due to continuous heat dissipation from the smoke to the colder tunnel walls and lower ambient air. Consequently, the influence of thermal buoyancy became less pronounced. As the velocity of the flow increased, the Froude number exhibited a corresponding increase. This is because the smoke experienced a more significant impact from inertial forces, while the effect of thermal buoyancy diminished. Fig. (7) shows temperature contours for the two fires as the longitudinal velocity increases from Fig. (7(a)) to Fig. (7(b)) for the 30MW fire, and from Fig. (7(c)) to Fig. (7(d)) for the 80 MW fire. In certain cases, the longitudinal velocity led to increased instability of the smoke near the fire source, resulting in a slightly higher Froude number in the vicinity of the fire source compared to the region further away from the fire source. This observation was particularly noticeable when considering parameters such as a heat release rate (HRR) of 30 MW and a velocity of 4 m/s.

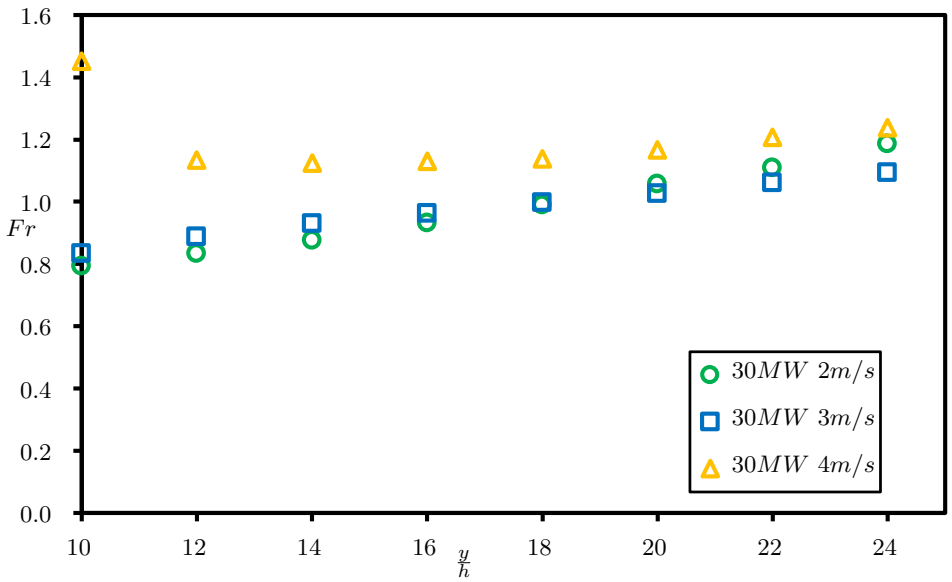


Fig. 6: Distribution of Froude numbers downstream from the fire source under different conditions for a 30MW fire.

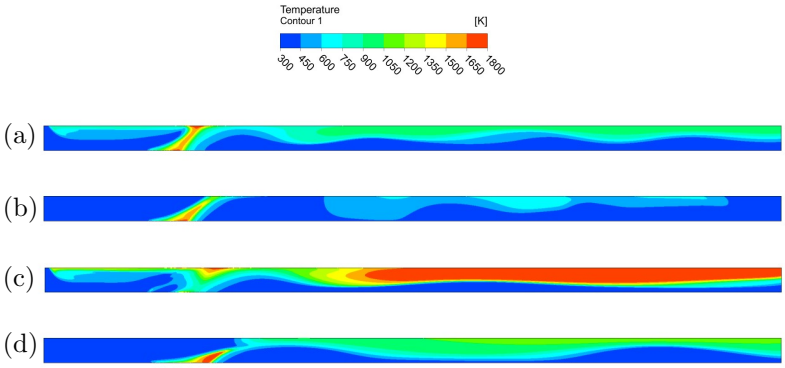


Fig. 7: Temperatures contours (a) for a 30MW fire under $u_0 = 2m/s$ ($Fr_{avg} = 1.0$), (b) for a 30MW fire under $u_0 = 4m/s$ ($Fr_{avg} = 1.2$), (c) for an 80 MW fire under $u_0 = 2m/s$ ($Fr_{avg} = 2.2$), and (d) for an 80 MW fire under $u_0 = 4m/s$ ($Fr_{avg} = 2.4$).

$\Delta T_{cf}/\Delta T_{avg}$ was plotted together with Fr in Fig. (8) and the resulting correlation with an R^2 value of 0.95 is shown in Eq. (13). This resulted in a critical Froude number value of $Fr_c = 0.858$. The reader is reminded that the critical Froude number in this study was evaluated at a criterion of $\Delta T_{cf}/\Delta T_{avg} = 1.9$, as opposed to 1.7 or 1.8 in previous studies. The new correlation in Eq. (13) is comparable to Newman's in Eq. (1) and the new critical Froude number of 0.858 is comparable to the 0.9 from Newman's experiments. It also agrees with $Fr_c \approx 1$ expected at the transition between stratification regimes.

$$\frac{\Delta T_{cf}}{\Delta T_{avg}} = 1.53 Fr^{-1.4} \tag{13}$$

Generally, the empirical correlations relating temperature ratio to Froude number seem to follow the general form of a power function shown in Eq. (14). The results from this study are compared to those from previous studies in Table 4.

$$\frac{\Delta T_{cf}}{\Delta T_{avg}} = A \times Fr^{-B} \tag{14}$$

Where A and B are empirical constants whose values are presented in Table 4.

While all studies presented here are focused on understanding the stratification of smoke and temperature layers in tunnels, they come up with different correlations and critical Froude numbers. However, there are similarities between this study and Newman [4], as well as between Nyman and Ingason [7] and Li et al. [8]. This study and Newman [4] both report similar empirical constants for A and B (1.53 vs. 1.5 for A and 1.4 vs. 1.0 for B, respectively). The critical Froude numbers (0.858 vs. 0.90, respectively) are also quite close, implying a similar transition point between

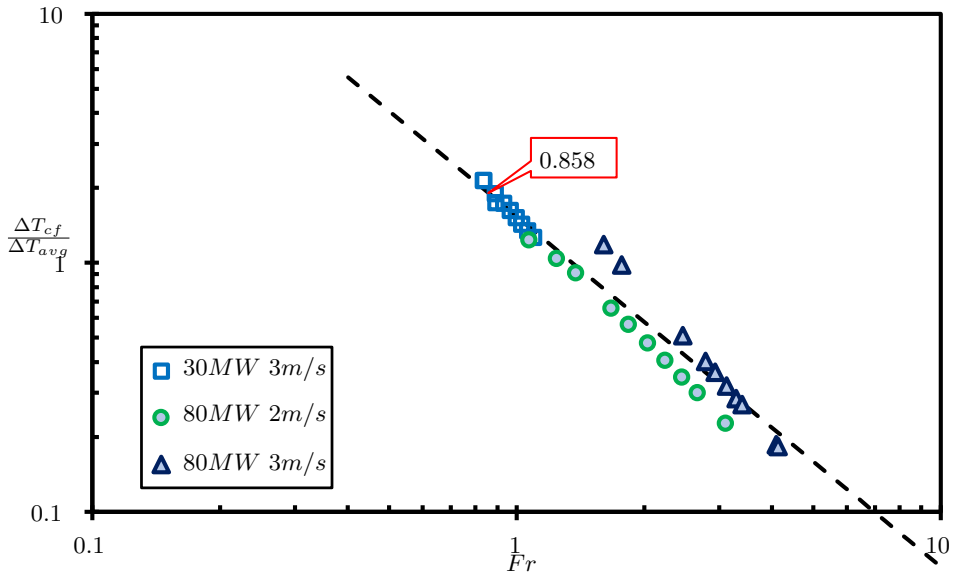


Fig. 8: The temperature ratio $\Delta T_{cf}/\Delta T_{avg}$ versus Froude number. The fitted correlation in Eq. (13) is plotted on the dotted line.

Table 4: Froude Number Correlations

A	B	Critical Fr	Reference
1.53	1.4	0.858	Current Study
1.5	1.0	0.90	Newman [4]
0.84	1.0	0.49	Guo et al. [10]
0.62	1.58	0.55	Nyman and Ingason [7]
0.67	1.54	0.55	Li et al. [8]
0.72	7.3	0.29	Huang and Li [9]

buoyancy and shear dominance. Nyman and Ingason [7] and Li et al. [8] both report similar values for A and B (0.62 and 0.67 for A, 1.58 and 1.54 for B, respectively), with an identical critical Froude number (0.55). All these studies are plotted together in Fig. (9).

Froude number has been widely adopted in tunnel fire research due to its apparent simplicity as a dimensionless parameter representing the ratio of inertial forces to buoyancy forces. In its temperature-based form, it is often expressed as:

$$Fr = u_{avg} \cdot (gh\Delta T_{cf}/T_{avg})^{-1/2}$$

This formulation has historical roots in the hydraulics of open-channel flows where it characterises the relationship between flow velocity and gravity wave propagation [30].

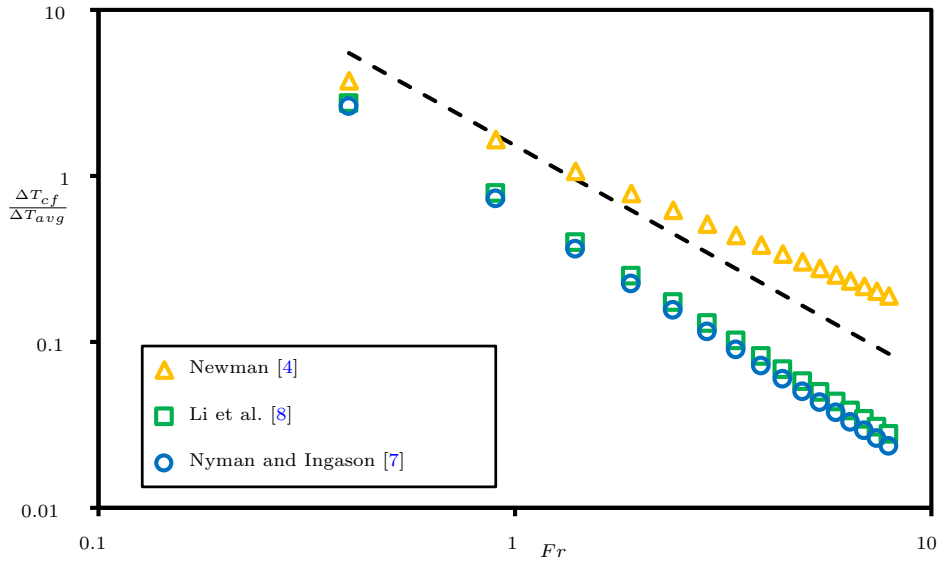


Fig. 9: Comparison of current study and previous results. The correlation from this study, shown in Eq. (13), is plotted on the dotted line.

However, the direct application of this single parameter to complex fire-driven flows presents limitations. The temperature-based Froude number does not account for local variations in the flow field, which is particularly relevant in large tunnel fires where thermal conditions vary significantly throughout the domain. Furthermore, the critical threshold of $Fr \approx 1$ does not apply universally in stratified shear flows; the transition between stratification regimes can occur at varying Froude numbers depending on the specific flow configuration and boundary conditions, as evidenced by the range of critical Froude numbers (0.29 to 1.63, shown in Table 4) reported in the literature. The Froude number implicitly assumes that stratification is governed by a two-force balance (inertia and buoyancy), whereas in reality the stability of stratification also depends on the local interplay between turbulence production and suppression, effects that a bulk parameter cannot capture. These limitations suggest that while the Froude number provides a useful first-order characterisation, it should be interpreted with caution, particularly for large fires where the thermal boundary conditions depart substantially from those of the small-scale experiments on which most correlations are based.

4 Conclusions

This computational study of thermal stratification in large tunnel fires provides several insights into fire-induced smoke behaviour under forced ventilation. The simulations demonstrate that large fires ($Q^* > 0.15$) generate floor temperatures significantly

exceeding ambient conditions, which means that the assumption of ambient floor temperature, common in small-scale fire studies, does not hold. The critical temperature ratio for stable stratification is found to be $\Delta T_{cf}/\Delta T_{avg} = 1.9$, higher than the traditionally accepted value of 1.7, with a corresponding critical Froude number of 0.858. An analytical estimate based on the assumption of ambient floor temperature yields a critical ratio of 2.0, which is closer to the value found here than to the conventional 1.7. A new empirical correlation relating the temperature ratio to the Froude number is proposed and shows good agreement with the seminal work of Newman [4]. The wide scatter in critical Froude numbers reported across the literature (0.29 to 1.63) underlines the sensitivity of this parameter to experimental configuration and fire scale. While the Froude number remains a practical first-order indicator of stratification stability, its limitations as a sole descriptor are evident, particularly for large fires where the thermal boundary conditions depart from those assumed in small-scale experiments. Future work employing scale-resolving simulations (e.g. LES or DNS) would be valuable for investigating the local turbulence dynamics that govern the transition between stratification regimes.

References

[1] Dhillon, B.: Global mine accidents. Mine safety: A modern approach, 59–71 (2010)

[2] Parks, M.: S. Africa Miners Strike to Protest Deadly Fire

[3] Yang, D., Hu, L.H., Huo, R., Jiang, Y.Q., Liu, S., Tang, F.: Experimental study on buoyant flow stratification induced by a fire in a horizontal channel. Applied Thermal Engineering **30**(8), 872–878 (2010)

[4] Newman, J.S.: Experimental evaluation of fire-induced stratification. Combustion and flame **57**(1), 33–39 (1984)

[5] Poreh, M., Marshall, N.R., Regev, A.: Entrainment by adhered two-dimensional plumes. Fire Safety Journal **43**(5), 344–350 (2008)

[6] Regev, A., Hassid, S., Poreh, M.: Density jumps in smoke flow along horizontal ceilings. Fire Safety J. **39**(6), 465–479 (2004)

[7] Nyman, H., Ingason, H.: Temperature stratification in tunnels. Fire safety journal **48**, 30–37 (2012)

[8] Li, L., Tang, F., Dong, M., Tao, C.: Effect of ceiling extraction system on the smoke thermal stratification in the longitudinal ventilation tunnel. Applied Thermal Engineering **109**, 312–317 (2016)

[9] Huang, D., Li, S.: An experimental investigation of stratification characteristic of fire smoke in the corridor under the effect of outdoor wind. Journal of Wind Engineering and Industrial Aerodynamics **179**, 173–183 (2018)

[10] Guo, Y., Yuan, Z., Yuan, Y., Cao, X., Zhao, P.: Numerical simulation of smoke stratification in tunnel fires under longitudinal velocities. Underground Space **6**(2), 163–172 (2021)

[11] Yang, L., Fan, C., Luan, D., Ouyang, R., Tao, H., Xu, Z., Wang, F.: Experimental study on thermal stratification characteristics in tunnel fires under the effect of canyon cross wind. Journal of Wind Engineering and Industrial Aerodynamics **218**, 104756 (2021)

[12] Li, Y.Z., Ingason, H.: The maximum ceiling gas temperature in a large tunnel fire. Fire Safety Journal **48**, 38–48 (2012)

[13] Li, Y., Lei, B., Ingason, H.: Scale modeling and numerical simulation of smoke control for rescue stations in long railway tunnels. Journal of Fire Protection Engineering **22**(2), 101–131 (2012)

[14] Ingason, H., Li, Y., Lönnermark, A.: Tunnel Fire Dynamics. Springer, ??? (2014)

[15] McGrattan, K., Hostikka, S., Floyd, J., McDermott, R., Vanella, M.: Fire Dynamics Simulator (version 6)–user's Guide vol. 1019, pp. 1–410. US Department of Commerce, Technology Administration, National Institute of Standards and Technology, ??? (2020)

[16] Shih, T.-H., Liou, W.W., Shabbir, A., Yang, Z., Zhu, J.: A new $\kappa - \epsilon$ eddy viscosity model for high reynolds number turbulent flows. Computers & fluids **24**(3), 227–238 (1995)

[17] Chui, E., Raithby, G.: Computation of radiant heat transfer on a nonorthogonal mesh using the finite-volume method. Numerical Heat Transfer **23**(3), 269–288 (1993)

[18] Li, Y.Z., Ingason, H.: Maximum ceiling temperature in a tunnel fire. SP report **51** (2010)

[19] Magnussen, B., Hjertager, B.: On mathematical modeling of turbulent combustion with special emphasis on soot formation and combustion. Symposium (international) on Combustion **16**(1), 719–729 (1977)

[20] Biffi, M., Stanton, D., Rose, H., Pienaar, D.: Ventilation strategies to meet future needs of the south african platinum industry. Journal of the Southern African Institute of Mining and Metallurgy **107**(1), 59–66 (2007)

[21] Ingason, H.: Fire dynamics in tunnels. The Handbook of Tunnel Fire Safety (2005)

[22] Hansen, R.: Design fires in underground mines (2010)

[23] Draper, D.: Assessment and propagation of model uncertainty. Journal of the

Royal Statistical Society Series B: Statistical Methodology **57**(1), 45–70 (1995)

[24] Li, C.W., Zhu, B.: A sigma coordinate 3d k–ε model for turbulent free surface flow over a submerged structure. Applied Mathematical Modelling **26**(12), 1139–1150 (2002)

[25] Wright, N.G., Easom, G.: Non-linear k–ε turbulence model results for flow over a building at full-scale. Applied Mathematical Modelling **27**(12), 1013–1033 (2003)

[26] Kechiche, J., Mhiri, H., Le Palec, G., Bournot, P.: Application of low reynolds number k–ε turbulence models to the study of turbulent wall jets. International Journal of Thermal Sciences **43**(2), 201–211 (2004)

[27] Van Maele, K., Merci, B.: Application of two buoyancy-modified k–ε turbulence models to different types of buoyant plumes. Fire Safety Journal **41**(2), 122–138 (2006)

[28] Davidson, L.: Calculation of the turbulent buoyancy-driven flow in a rectangular cavity using an efficient solver and two different low reynolds number κ-ε turbulence models. Numerical Heat Transfer **18**(2), 129–147 (1990)

[29] Gupta, A., Eswaran, V., Munshi, P., Maheshwari, N., Vijayan, P.: Thermal stratification studies in a side heated water pool for advanced heavy water reactor applications. Heat and mass transfer **45**(3), 275–285 (2009)

[30] Long, R.R.: Stratified Flow. Encyclopaedia Britannica Educational Corporation, ??? (1968)